

Scotland's Rural College

Stereological assessment of sexual dimorphism in the rat liver reveals differences in hepatocytes and Kupffer cells but not hepatic stellate cells

Marcos, R; Lopes, C; Malhao, F; Correia-Gomes, C; Fonseca, S; Lima, M; Gebhardt, R; Rocha, E

Published in:
Journal of Anatomy

DOI:
[10.1111/joa.12448](https://doi.org/10.1111/joa.12448)

First published: 01/01/2016

Document Version
Peer reviewed version

[Link to publication](#)

Citation for pulished version (APA):

Marcos, R., Lopes, C., Malhao, F., Correia-Gomes, C., Fonseca, S., Lima, M., Gebhardt, R., & Rocha, E. (2016). Stereological assessment of sexual dimorphism in the rat liver reveals differences in hepatocytes and Kupffer cells but not hepatic stellate cells. *Journal of Anatomy*, 228(6), 996 - 1005. <https://doi.org/10.1111/joa.12448>

General rights

Copyright and moral rights for the publications made accessible in the public portal are retained by the authors and/or other copyright owners and it is a condition of accessing publications that users recognise and abide by the legal requirements associated with these rights.

- Users may download and print one copy of any publication from the public portal for the purpose of private study or research.
- You may not further distribute the material or use it for any profit-making activity or commercial gain
- You may freely distribute the URL identifying the publication in the public portal ?

Take down policy

If you believe that this document breaches copyright please contact us providing details, and we will remove access to the work immediately and investigate your claim.

1 Stereological assessment of sexual dimorphism in the rat liver reveals differences in
2 hepatocytes and Kupffer cells but not hepatic stellate cells

3
4 Ricardo Marcos^{1,2}, Célia Lopes^{1,2}, Fernanda Malhão^{1,2}, Carla Correia-Gomes³, Sónia
5 Fonseca⁴, Margarida Lima⁴, Rolf Gebhardt⁵, Eduardo Rocha^{1,2}

6
7 ¹ Laboratory of Histology and Embryology, Department of Microscopy, ICBAS -
8 Institute of Biomedical Sciences Abel Salazar, U.Porto - University of Porto, Portugal

9 ² Histomorphology, Physiopathology and Applied Toxicology Group, CIIMAR -
10 Interdisciplinary Centre of Marine and Environmental Research, U.Porto, Portugal

11 ³ Scotland's Rural College, Epidemiology Research Unit- Future Farming Systems
12 Group. Inverness, United Kingdom.

13 ⁴ Laboratory of Cytometry, Department of Hematology, HSA – Hospital de Santo
14 António, CHP – Centro Hospitalar do Porto, UMIB – Unit for Multidisciplinary
15 Research in Biomedicine, ICBAS - Institute of Biomedical Sciences Abel Salazar,
16 U.Porto - University of Porto, Portugal.

17 ⁵ Institute of Biochemistry, Faculty of Medicine, University of Leipzig, Leipzig,
18 Germany.

19
20 Running title: Male versus female differences in the liver.

21
22 Keywords: Hepatic stellate cells, Kupffer cells, hepatocytes, liver, dimorphism,
23 stereology.

24
25 Corresponding author: Ricardo Marcos (DVM, MD, PhD)

26 Laboratory of Histology and Embryology
27 Institute of Biomedical Sciences Abel Salazar
28 Rua de Jorge Viterbo Ferreira no. 228,
29 4050-313 Porto, Portugal
30 Email: rmarcos@icbas.up.pt

Abstract

There is long-standing evidence that the male and female rat liver differ in enzyme activity. More recently, differences in gene expression profiling have also been found to exist; however, it is still unclear whether there is morphological expression of male/female differences in the normal liver. Such differences could help to explain features seen at the pathological level, such as the greater regenerative potential generally attributed to the female liver. In this paper, hepatocytes (HEP), Kupffer cells (KC) and hepatic stellate cells (HSC) of male and female rats were examined to investigate hypothesized differences in number, volume and spatial co-localization of these cell types. Immunohistochemistry and design-based stereology were used to estimate total numbers, number per gram and mean cell volumes. The position of HSC within lobules (periportal versus centrilobular) and their spatial vicinity to KC was also assessed. In addition, flow cytometry was used to investigate the liver ploidy. In the case of HEP and KC, differences in the measured cell parameters were observed between male and female specimens; however, no such differences were detected for HSC. Female samples contained a higher number of HEP per gram, with more binucleate cells. The HEP nuclei were smaller in females, which was coincident with more abundant diploid particles in these animals. In the case of KC, the female liver also had a greater number per gram, with a lower percentage of KC in the vicinity of HSC compared to males. In this study, we document hitherto unknown morphological sexual dimorphism in the rat liver, namely in HEP and KC. These differences may account for the higher regenerative potential of the female liver and lend weight to the argument for considering the rat liver as a sexually dimorphic organ.

Introduction

Biological inequality is related to so-called gender or sexual dimorphism, in which females have an increased resistance to premature ageing, nutrient deprivation, vascular and heart diseases, brain disorders, as well as hepatic neoplasms and hepatitis C virus infection (Li et al. 2012; Grebely et al. 2014). Evidence has mounted over the past thirty years to demonstrate that the mammalian liver is responsive to steroid sex hormones. These can modulate many functional features of the organ; apart from the differences in cytochrome-P-450, diverse contents of glucose-6-phosphatase (Teutsch, 1984), glutamine synthetase (Sirma et al. 1996) and lipogenic enzymes (Scheicher et al. 2015) have been reported. Pathological features are also modulated by sex hormones, illustrated by the fact that progression to cirrhosis in men can occur at a rate 10-times faster than that seen in women (Poynard et al. 2001; Massard et al. 2006; Villa, 2008). *In vitro* studies showed that oestrogens have antioxidant properties, reducing proliferation and collagen synthesis in cultured hepatic stellate cells (HSC) (Yasuda et al. 1999). There is no doubt that, at first sight, the microscopic morphology of the liver appears similar in both sexes; however, it is unknown whether male and female HSC differ in volume, number, surrounding cells or position within the liver lobules. Since HSC are deeply influenced by the surrounding milieu (Kmieć, 2001), such differences would explain, at least partially, the faster progression of collagen deposition in males. The liver also exhibits sexual dimorphism in its capacity to regenerate. Unlike most organs, the liver can increase its cell numbers after injury, restoring the lost mass to obtain its optimal volume. Experimental studies in rats have shown a higher degree of regeneration in females (Tsukamoto & Kojo 1990; Biondo-Simões et al. 2006; Kitagawa et al. 2009) and the scarce clinical data in humans also points in the same direction (*e.g.*, Imamura et al. 1999). Liver regeneration is of utmost importance in liver transplantation, namely when “small for size” grafts are used. Among the many proliferation factors, the “augmenter of liver regeneration” is an enigmatic protein released by hepatocytes (HEP) that promotes liver growth (Gandhi, 2015). Recently, it was shown that hepatocellular proliferation depends on the integrity of the Kupffer cells (KC), since their depletion with gadolinium chloride significantly reduced the increase in organ weight, as well as survival after small-for-size transplantation among a cohort of rats (Yang et al. 2013). Still, the ratio of KC to HEP remains scarcely studied (Santos et al. 2009), and it remains unknown if this ratio differs between the sexes. Intersexual

differences in HEP and KC could help to explain the increased risk of graft loss in female-to-male liver transplants (Lai et al. 2011; Croome et al. 2014).

A potential mechanism behind the dimorphic liver regeneration is related to ploidy differences, since diploid HEP are known to divide more rapidly than polyploid cells after hepatectomy (Gupta, 2000). Cell ploidy is classically related to the cell volume (Epstein, 1967), but male versus female differences in this parameter have never been detailed by morphometry or stereology. Nevertheless, it would be interesting to relate such data to DNA staining with propidium iodide and flow cytometry, which are well recognized tools to evaluate ploidy, based on cell DNA content (Gupta, 2000).

In view of the state of the art, we hypothesized that there are structural differences in the normal liver of males and females that could help explain differences in pathological scenarios. To help elucidate the hypothesis, we combined design-based stereology and flow cytometry to disclose sexual dimorphism in selected targets cells of the rat liver. We first checked if significant differences existed in collagen in the lobules, the main endpoint of HSC activity. Apart from evaluating the total number and number per gram, we looked at the volume and intralobular position of these cells. Since it is recognized that the first fibrogenic stimulus is modulated by KC, we not only estimated their total number and number per gram but also quantified their vicinity to HSC. Moreover, we also examined the numbers and percentage of binucleate hepatocytes (BnHEP), as well as their cell and nuclear volume. The latter data enabled us to better evaluate, by a morphological approach, if differences in ploidy existed across males and females. These were later evaluated by a flow cytometry approach.

Materials and Methods

Animals

We used male and female Wistar rats ($n = 5$ per group) aged 2 months old, bought from Charles-River Laboratories (Barcelona, Spain). All animals had been weaned at 20 days and kept in standard conditions, receiving water and food ad-libitum in a controlled environment [temperature of 25 °C and 12 hours alternated light-dark cycles, with light period starting at 7.00 AM]. Males weighed 351 ± 17 g and females 216 ± 13 g. The management of animals and procedures followed the European Union Directives (1999/575/CE and 2010/63/UE) for the protection of animals used for scientific purposes.

Tissue Preparation

Sampling was performed during the morning period (from 10 to 12 AM), to circumvent oscillations in liver functions due to circadian rhythmicity (Davidson et al. 2004). In females, daily vaginal cytologies were observed, in order to avoid collecting samples in proestrous/oestrous days. Beforehand, animals were deeply anaesthetised with ketamine plus xylazine and blood was collected from the heart and centrifuged to obtain serum for assessing alanine and aspartate transaminase levels. Transcardiac perfusion was performed for 15 minutes with an isosmotic solution, the liver was weighed and its volume determined by the Scherle's method, as detailed elsewhere (Marcos et al. 2012). A smooth fractionator sampling scheme was applied: half of the paraffin blocks were used for thick sections (30 μ m thick) and exhaustively sectioned in a motorised microtome, whilst the other half were used for thin sections (3 μ m thick) (Fig. 1). In thick sections, we sampled five sections in every 30, which were immunostained against: 1) glial fibrillary acidic protein for estimating the total number and number per gram of HSC; 2) ED2 for estimating these parameters in KC; 3) E-cadherin, to differentiate mononucleated from BnHEP, estimating their percentage, and assessing the total number and number per gram of HEP; 4) glial fibrillary acidic protein and glutamine synthetase [an established marker of centrilobular HEP (Gebhardt & Mecke 1983)], to evaluate the lobular distribution of HSC; 5) glial fibrillary acidic protein and ED2 to study the vicinity between HSC and KC. As to the thin sections, these were used for immunohistochemistry against glial fibrillary acidic protein, to determine the relative volume of HSC, and for histochemical staining with Sirius red, to assess the relative volume of fibrous tissue (Fig. 1).

Thick Sections

Immunohistochemistry

The protocol used for thick sections has been previously described (Marcos et al. 2004; 2006). Briefly, antigen recovery was carried out in a microwave (four plus four minutes, at 600 W) and a streptavidin-biotin protocol was used (Histostain Plus, Invitrogen, Camarillo, California). For glial fibrillary acidic protein, we used 1:3000 rabbit polyclonal antibody (Dako, Glostrup, Denmark), whereas for ED2 and E-cadherin we used monoclonal mouse antibodies, from Serotec (United Kingdom) diluted at 1:100 and from Dako (clone NCH 38) diluted at 1:250, respectively. All slides were incubated for four days at 4°C.

Slides for double immunohistochemistry were also placed in the microwave (this time for three cycles of four minutes). After blocking endogenous biotin and peroxidase, the first streptavidin-biotin protocol followed, with antibody against glial fibrillary acidic protein (1:1500 dilution for four days at 4°C). Slides were developed for two minutes in 0.05% 3,3'-diaminobenzidine (Dako) in Tris-buffered saline with 0.03% H₂O₂ and were then rinsed in tap-water and dipped in 50 mM glycine buffer (pH = 2.2) for five minutes, to strip off the antibodies of the first immunoreaction. The second streptavidin-biotin protocol followed, using 1:4000 rabbit polyclonal antibody against glutamine synthetase (kindly gifted by Professor Rolf Gebhardt, University of Leipzig), for another four days at 4°C. Slides were developed with aminoethylcarbazole (Dako) for 10 to 20 minutes (the final red colour was controlled by microscopic observation) and slides were mounted in Aquatex (Dako). Regarding the double immunohistochemistry to evaluate the vicinity of HSC and KC, the protocol was similar to the above described, except for the second antibody (ED2 at 1:100 dilution).

Stereological Analysis

We used a stereology workstation detailed elsewhere (Marcos et al. 2004) with an Olympus CAST-Grid software (version 1.5, Olympus). At the monitor, a final magnification of 4750x allowed an easy and accurate recognition of all cells. Throughout the disector height (20 µm), a software-generated counting frame was superimposed with defined areas (1673 µm², 1267 µm² and 418 µm² for HSC, KC and HEP, respectively). In the slides used for assessing the position of HSC within the lobule, a systematic uniform random sampling was also used, but HSC were counted

only if fields were in the vicinity of the portal tracts or central venules (we settled these areas as 5-6 HEP around these landmarks). For the double immunohistochemistry of HSC and KC, the largest counting grid was used and a minimum of 100 HSC were evaluated per animal (Fig. 2).

For counting cells, the nucleus was selected as the counting unit (in the case of BnHEP, this was predetermined to be the first nucleus appearing in focus). Cells were counted following the optical disector rules (Marcos et al. 2004; 2006). The potential bias from lost caps was avoided by having upper and lower guard heights, which have previously been validated for the rat liver (Marcos et al. 2012). The collapse in the z -direction was also evaluated, by measuring the full section thickness with the microcator in every fifth field (Dorph-Petersen et al. 2001).

The total number of HSC, KC and HEP in the whole liver was primarily estimated according to the optical fractionator rules, meaning that the inverse of block, section, area and height sampling fraction were multiplied by the number of cells counted in the disectors (Marcos et al. 2012). Simultaneously, the number per gram was determined, as this can aid when comparing values between animals with different liver weights. The coefficient of error of the number of cells counted was estimated, using formulae described elsewhere (Marcos et al. 2004).

Additionally, the number-weighted mean cell and nuclear volume of mononuclear and BnHEP was estimated by the nucleator method (Gundersen, 1988; Marcos et al. 2012). In this case, HEP were firstly sampled by the optical disector and their nucleolus selected. Afterwards, the software generated two isotropic lines from the nucleolus and the intersections between these lines and nuclear and cell borders were marked. The average distance from the intersections to the nucleolus was used to estimate the number-weighted mean cell and nuclear volume. In the case of HEP with two nucleoli (or more), the measurements were performed for the two (or more) particles (Gundersen, 1988).

Positive and negative controls (omission of first antibody and replacement by non-immune serum) were included, both in thin and thick sections, and all slides were blindly evaluated (*i.e.*, the observer was unaware of the sex of the animal), in order to avoid eventual observer-related bias.

Thin Sections

Immunohistochemistry

A streptavidin–biotin protocol was also used (Histostain Plus) for glial fibrillary acidic protein immunostaining. In this case, shorter incubation times were needed: the antibody was diluted to 1:1200 and incubated overnight, whilst the blocking solution, secondary antibody and streptavidin–peroxidase complex were all applied for 20 minutes; colour development in DAB was restricted to two minutes.

Histochemical Sirius red staining

Thin sections were counterstained with celestial blue and Mayer's haematoxylin, each for five minutes; then, after washing in tap water, the Sirius red (Sigma, coloration index 35782) dissolved in picric acid (1 mg/ml) was applied for one hour at room temperature (Junqueira et al. 1978). After washing in acidified water (1% acetic acid), sections were dehydrated, cleared and mounted.

Stereological analysis

Five sections were randomly selected per animal and an average of 150 oil-immersion fields were quantified per animal (fields were “selected” after systematic uniform random sampling performed by the software). A test-system of points was superimposed by the software in order to determine the relative volume of HSC in the slides immunostained against glial fibrillary acidic protein (Fig. 3). The test-system included 12 sparser points, used to quantify the reference space (whole liver) and 108 denser ones used for HSC. The relative volume of HSC was estimated as a ratio of the two sets of points (Marcos et al. 2012). This parameter was multiplied by the liver volume and divided by the total number of HSC in order to estimate the number-weighted mean cell volume of HSC (Marcos et al. 2012).

The amount of collagen in Sirius red stained slides was also evaluated by a similar strategy, but with 40x magnification lens (rendering a final magnification of 1600x at the screen) and a scanner test system of 36 points (which was judged adequate to estimate the relative volume of collagen). Point counting was used to determine the relative volume of fibrous tissue (collagen I and III) in the liver, focusing on three different locations: 1) Glisson's capsule; 2) vascular (portal spaces and around central veins); 3) intralobular (surrounding sinusoids).

Flow cytometry

In order to determine ploidy differences, liver pieces (≈ 0.7 g) frozen at -80°C were gently thawed in phosphate buffered saline ($\text{pH} = 7.4$), and mechanically disaggregated with tweezers. The homogenate was centrifuged at 750 G for five minutes, and the supernatant decanted. The pellet was suspended in phosphate buffered saline and the cell yield calculated in a haematology analyser (LH 780, Beckman Coulter, Brea, California). Afterwards, the suspension was split into two parts: one for cytological examination (cytospins) and the other for flow cytometry. For the latter, one 100 μl aliquot of each sample (with an average of 3×10^6 cells/ μl) was stained using the Coulter DNA-Prep Reagents Kit (Beckman Coulter), according to the manufacturer's instructions. This was performed by sequentially dispensing and mixing 100 μl of the lysing and permeabilising reagent (DNA Prep LPR), and 1 ml of the staining solution containing 50 $\mu\text{g/ml}$ propidium iodide and 4 KU/ml bovine pancreas type III RNAase (DNA Prep Stain) and finally, samples were incubated for 20 minutes in the dark. For the flow cytometry analysis a Coulter EPICS-XL-MCL (Beckman Coulter) with a 488 nm argon ion laser was used. Sample acquisition was performed for a minimum of 30 minutes and a minimum of 20,000 events per sample were acquired. Rat lymphocytes were employed as a control for diploid cells. Analysis was performed with the MultiCycle software (Phoenix Flow Systems, San Diego), with modified exponential debris function. The percentage of diploid, tetraploid and octaploid particles was assessed.

Statistical analysis

The software SPSS 18 (IBM, Armonk, United States of America) was used. After checking if the data followed a normal distribution with the Shapiro-Wilk's test, a correlation analysis was conducted to detect linear correlations. Subsequent to assessing the homogeneity of variances (Levene's test), the Student's t-test for unpaired samples was used for comparing the means from males and females. In the case of liver weight, relative volume of collagen and variables related with HSC (total number, number per gram, number-weighted mean cell volume and lobular distribution), the non-parametric equivalent, Mann-Whitney's U-test, was used for comparing medians from males and females. Significance level was set at $p \leq 0.05$.

Results

Livers displayed a normal morphology, without noticeable differences across animals. The livers of males were significantly heavier ($p = 0.02$) than those of females (14.11 ± 2.9 g versus 9.75 ± 0.7 g, respectively). Likewise, male livers were significantly larger. The liver-to-body weight ratio was 4.0 ± 0.7 % and 4.5 ± 0.6 % in males and females, respectively. A very strong correlation was observed between liver and body weight ($r = 0.8$; $p = 0.01$). Hepatic transaminases values were within the reference ranges (14-80 IU/L for alanine and 40-383 for aspartate transaminase levels), presenting no significant differences (42.0 ± 5.6 IU/L and 29.3 ± 10.9 IU/L for alanine and 98.8 ± 52.8 IU/L and 88.0 ± 42.2 IU/L for aspartate transaminase in males and females, respectively).

Thick sections

An average of 509 and 273 disectors were analysed for male and female rats, respectively. The total number of HSC was significantly higher in males than in females ($p = 0.016$), but their number per gram was similar (Table 1). By way of contrast, the total number of HEP was similar in males and females, although the latter had a significantly higher number per gram ($p = 0.016$). The same was seen for the BnHEP and KC: where the number per gram was significantly higher in females ($p = 0.016$), but the total number was similar in both sexes. The proportion of BnHEP, was 24.8 ± 4.2 % for males and 33.8 ± 4.7 % for females indicating no significant difference. It is noteworthy that the coefficient of error of the number estimations of HSC, HEP and KC was low, being between 0.039 and 0.060. This means that the methodological variability contributed much less to the total variance than the biological component (the latter was responsible for 80-93% of the total variance).

A very strong correlation was observed between the total number of HSC and liver weight ($r = 0.85$, $p = 0.004$). In addition, the number per gram of HEP was also correlated with that of KC and with the number per gram of BnHEP ($r = 0.94$, $p < 0.001$ and $r = 0.75$, $p = 0.02$, respectively). The relative volume of intralobular collagen was correlated only with the total number of HEP ($r = 0.74$, $p = 0.037$) — this correlation was mainly with mononucleated HEP, since no correlation existed with the number of BnHEP. As to the percentage of BnHEP, it was negatively correlated with the body weight ($r = -0.81$, $p = 0.015$) and total number of HEP ($r = -0.76$, $p = 0.028$).

The number-weighted mean cell and nuclear volume of HEP were also evaluated; on average, 107 HEP per animal were assessed for these purposes (Table 2). Male versus

female differences existed for mononucleated HEP ($p = 0.002$), but not for BnHEP. Mononucleated cells were 21% to 34% smaller than BnHEP ($p < 0.001$). With regard to the number-weighted mean nuclear volume, significant male/female differences existed for mononucleated HEP ($p = 0.029$). The histogram of the number-weighted mean nuclear volume revealed small differences: young females exhibited a slightly skewed pattern (Pearson's skewness = 1.0; kurtosis = 3.38) compared to males (Pearson's skewness = 0.34; kurtosis = 0.51) (Fig. 4). Considering that the histogram featured two modes, observed in data from both females and males, we computed this as two distributions (one for diploid cells and the other for tetraploid cells). The first mode was considered the mean of the diploid cells and the second the mean of the tetraploid cells. The standard deviation for each group was calculated based on the means. In this way, we estimated the number-weighted mean nuclear volume of the diploid nuclei as $225 \pm 36 \mu\text{m}^3$, whereas the tetraploid nuclei had a mean volume of $447 \pm 52 \mu\text{m}^3$. The number-weighted mean nuclear volumes of mononucleated HEP and BnHEP were not significantly correlated with their respective cell volumes ($p = 0.085$ and 0.072 , respectively). In BnHEP, the two nuclei presented volumes of the same order of magnitude, but the coefficient of variance between nuclei varied up to 14%. The nuclear to cytoplasm ratio was between 9.2% and 11.9% and no differences existed between mononucleated and BnHEP.

For the distribution of HSC in liver lobules, we evaluated an average of 303 HSC per animal and cells were significantly more abundant in centrilobular regions ($56.5 \pm 4.5\%$) than in periportal locations ($43.3 \pm 4.3\%$) ($p = 0.001$). The distribution of cells was similar in males and females and no staining intensity differences could be detected between these locations. As to cells neighbouring HSC, we should stress that the thick sections, encompassing all KC and HSC cell processes, allowed easy recognition of cell juxtapositions (Fig. 2). On average, we evaluated 188 HSC per animal, noting that $41.6 \pm 6.7\%$ were physically positioned next to KC in males. In females a lower number of HSC ($26 \pm 7.4\%$) had KC for neighbours; the difference in the position of these two cells was statistically significant ($p = 0.001$).

Thin sections

An average of 216 fields was screened per animal. In males, the intralobular collagen corresponded to 56% of the total collagen, whereas 20% and 14% were located in portal tracts and around central venules respectively and only 10% was found in the Glisson's

capsule. A similar scenario existed in females: 46 % was intralobular, 42% around vessels (respectively, 28% and 14% in a portal and central location) and 12% in the capsule. No significant differences existed in these proportions between males and females. As to the collagen content in the liver, no differences existed between males ($2.05 \pm 0.2\%$) and females ($1.95 \pm 0.3\%$).

In thin paraffin sections we also evaluated the relative volume of HSC immunostained by glial fibrillary acidic protein (Fig. 3). No statistical differences existed for this parameter across the sexes (Table 1). Regarding the number-weighted mean cell volume of HSC, no statistical differences were noted: male and female HSC had $619 \pm 128 \mu\text{m}^3$ and $786 \pm 192 \mu\text{m}^3$, respectively.

Flow cytometry

The mechanical dissociation of the liver rendered a mixture of particles, mostly formed by HEP nuclei (easily identified by their large size and presence of nucleoli) and well preserved HEP (both mononucleated and BnHEP), in variable proportions. Owing to the mechanical dispersion of the liver cells and to the washing procedure, followed by slow speed centrifugation, non-hepatocytes were present in low numbers (an average of less than 5% of the nuclei, as verified by light microscopy, in the cytopsin smears).

The flow cytometry analysis showed that the percentage of diploid particles (i.e., naked nuclei with 2N mixed with cells with 2N) tended to be more abundant in females (Table 3): significant differences existed between males and females ($p = 0.02$). No octaploid particles were observed.

Discussion

In this paper, we document, for the first time, the existence of linear correlations across liver cells. Apart from the strong correlation between the liver weight and the total number of HSC, these were also correlated with HEP; furthermore, correlations were established with BnHEP and KC. This emphasizes the complex functional interplay that takes place in the liver, which will be discussed below, cell by cell.

Hepatic stellate cells

Since liver fibrosis differs across sex in humans and rats, it could be hypothesized that baseline microanatomical differences in HSC exist in the normal organ. However, this was not backed by our data, as no quantitative differences were observed.

With regard to collagen deposition, a well recognized end-product of HSC (Friedman, 2008), no sexual differences exist and this is in accordance with previous studies that estimated collagen via hydroxyproline content (*e.g.*, Shimizu et al. 1999). Our estimation of the relative volume of collagen and its distribution in the liver are also in accordance with previous studies (Harkness & Harkness 1954; Gascon-Barré et al. 1989). The synthesis of extracellular matrix and collagen in normal liver is ascribed to various cell types besides HSC, including HEP and liver sinusoidal endothelial cells (Friedman, 2008), but surprisingly, of the three cell types examined here, we found a correlation only with HEP. This suggests that these cells may be the most relevant for collagen production in a normal setting, contrasting with cirrhotic livers, in which HSC have a leading role (Gressner & Weiskirchen 2006).

The mean cellular volume of HSC has, to the best of our knowledge, never been reported. In this study, we opted for an indirect approach to estimate the number-weighted mean cell volume, because local estimators (for instance the nucleator) would be extremely difficult to implement. HSC have cellular extensions expanding in various directions (Oikawa et al. 2002) that would be in and out of focus in thick sections. It should be noted that our estimation ($\approx 700 \mu\text{m}^3$ in males and females) is satisfactory for practical purposes but represents a slight underestimation, because we highlighted the cytoskeleton and not the cell borders. Regarding volume estimation and HSC, the single study that estimated their relative volume obtained values of $0.4 \pm 0.1\%$ (Martin et al. 1992a), which is comparable to our figure ($0.3 \pm 0.1\%$).

The lobulation of HSC has never been studied by stereology but has been a controversial topic. Herein, we reported a pericentral predominance in both males and

females, but Wake (1980) and Geerts et al. (1991) — using vitamin A autofluorescence and immunohistochemistry against desmin, respectively — reported a periportal predominance. Nevertheless, Higashi & Senoo (2003) and Senoo et al. (2007) used similar methods but found no lobular differences. The fact that we used antigen retrieval and long incubation times in paraffin sections (in contrast with cryostat sections of most studies) probably accounts for the differences. Moreover, a stereological strategy in thick sections should be more reliable for quantifying lobular heterogeneity, since thin sections viewed at low magnification naturally tend to a bias towards periportal areas, which are far more cellular (Teutsch et al. 1999).

Hepatocytes

Sexual differences in HEP have never been evaluated by quantitative morphology, as far as we are aware. Regarding their total number, we did not observe significant male/female differences — even if they could be expected due to the geometric scaling related to a larger liver and body size of males. Surprisingly, sexual dimorphism was evident when assessing number of HEP per gram, the so-called hepatocellularity. This parameter is important, not only because it allows a straightforward comparison between studies, but also because it is widely used when *in vivo* hepatic clearance needs to be predicted (Barter et al. 2007). Using different methodologies, hepatocellularity in the male rat has ranged from 85×10^6 HEP per gram (Carlile et al. 1997) to almost double that figure at 163×10^6 HEP per gram (Smith et al. 2008); in humans, the value of 120×10^6 HEP per gram has been predicted from the study of liver microsomes (Hirota et al. 2001). Sexual differences have been rarely considered, but Atchley et al. (2000) proposed their existence in mice (after puberty), with females having significantly more and smaller HEP than males; overall, this is in accordance with our data. The higher hepatocellularity in females may be explained by effects of oestrogens, since, at least *in vitro*, ethinylestradiol has induced a 7-fold increase in HEP proliferation, with DNA synthesis, but without cytotoxicity or induction of cytochrome-P-450 (Vickers and Lucier 1996). A pioneer study by Fisher et al. (1984) also showed that the livers of female rats receiving multiple injections of estradiol were 27% heavier and had an increase of total DNA.

We highlighted a negative correlation between BnHEP percentage and body and liver weight. A negative correlation between binuclearity, nuclear ploidy and body weight

seems to be a feature of mammals, including rats (Vinogradov et al. 2001). It has been known for more than sixty years (St Aubin & Bucher 1952) that the percentage of BnHEP decreases whilst the total number of HEP increases during normal rat growth and in partial hepatectomy. This phenomenon is also suggested by our data, by the negative correlation between the percentage of BnHEP and the total number of HEP. Even if no sexual differences existed in the percentage of BnHEP, we observed significant differences in their number per gram. This could be related to insulin, since *in vitro* studies have demonstrated that epidermal growth factor and insulin induced a high rate of BnHEP, similar to that normally observed in the liver of growing rats (Mossin et al. 1994). More recently, it was reported that rats with low insulin levels had less formation of BnHEP compared to animals injected with the hormone (Celton-Morizur & Desdouets 2010). Interestingly, differences in insulin also appear to exist in normal rats with higher levels in females (Da Costa et al. 2004; Vital et al. 2006). Oestrogens may also play a role here, since oophorectomised rats have significantly lower insulin levels that can be restored with estradiol administration (Ahmadi & Oryan 2008). The functional significance of sexual dimorphism in the number per gram of HEP and BnHEP is still unknown, but it may underlie the larger functional reserve and the higher regenerative potential reported for the female liver (Shimizu et al. 2007).

Another interesting finding of our study relates to the volume of HEP. It is often assumed that BnHEP are twice the size of mononucleated HEP (*e.g.*, Celton-Morizur & Desdouets 2010; Crawford & Burt 2012). Since a twofold increase in volume corresponds to only a 1.4-fold increase in surface area, this would result in less efficient transport in BnHEP (Pandit et al. 2013). The twofold assumption has been substantiated by classical studies which dissociated HEP mechanically (Epstein, 1967, Martin et al. 1992b). It should be noted that isolated HEP tend to enlarge, because they do not have compressive forces of adjacent cells and they often appear flattened (and further enlarged) bellow the coverslip (St Aubin & Bucher 1952). Our data strongly contradicts a twofold proportionality because the number-weighted mean cell volume of BnHEP is only 25% to 37% larger than that of mononucleated HEP and no correlation existed between the number-weighted mean cell volume of these cells. In fact, the use of different meshes to sort HEP after isolation has already showed that cell size is not correlated with binuclearity or ploidy (Gandillet et al. 2003).

It should be emphasized that the number-weighted mean cell volume of HEP is an important parameter in research, being considered the best predictor of liver cancer in

rodents (Hall et al. 2012). Overall, our data on the volume of HEP is coincident with general figures reported [5000 to 6000 μm^3 (McCuskey, 2006, Grisham, 2009)] and closely resembles those of Jack et al. (1990), who also used stereological methods.

Kupffer cells

To the best of our knowledge, this is the first report of sexual dimorphism in the number per gram of KC. Notably it has been shown that female rats as well as mice have $\approx 50\%$ more macrophages than males, both in their pleural and peritoneal cavities, with more toll-like receptors and more efficiency in phagocytosis (Scotland et al. 2011). Even if new numerical differences were disclosed herein, it has been known for a long time that KC are influenced by oestrogen: peaks of phagocytosis and proliferation have been correlated with elevated oestrogen in the oestrous cycle of mice and rats (Nicol & Veron-Roberts 1965; Vickers and Lucier 1996).

The HSC-KC vicinity should favour the crosstalk and paracrine/juxtacrine stimulation among these cells, which is nowadays viewed as reciprocal (Tacke and Zimmermann 2014). Since liver sinusoids have fenestrae it is easy for intrasinusoidal KC to contact directly with perisinusoidal HSC. The relationship between these cells has a long history; it has been known for more than 25 years that the conditioned medium of KC is able to stimulate collagen synthesis and activation of HSC (Friedman & Arthur 1989), whereas HSC-derived molecules promote the differentiation of a more pro-inflammatory and pro-fibrotic phenotype of KC (Chang et al. 2013). Because sexual differences exist in the constellation of HSC-KC — viz. $41.6 \pm 6.7\%$ and $26 \pm 7.4\%$ in males and females, respectively — it could be hypothesized that a less pro-inflammatory KC phenotype could be present in the female rat liver.

In conclusion, we have demonstrated that HEP and KC, but not HSC, have significant sexual dimorphism. This may be due to oestrogens acting in receptors α , which functionally exist in HEP and KC but not in HSC (Shimizu et al. 2007). In view of the fact that mechanisms underlying clinically sexual dimorphism are largely unknown (Yokoyama et al. 2007; Li et al. 2012), this study adds substantial understanding by showing that primal morphological quantitative differences do exist in the rat liver. This should be taken into account when planning studies and interpreting sexual-differences in liver regeneration, inflammatory and fibrotic conditions. In addition, it would be particularly interesting to investigate whether our findings in rats also apply to humans.

Acknowledgments

This work was financially supported by FEDER funds through the Competitiveness and Trade Expansion Program (COMPETE) and by national funds, Fundação para a Ciência e Tecnologia (FCT) via a doctoral grant (SFRH/BD/38958/2007). We are deeply grateful to Madelaine Henry for English language editing.

Conflict of interest

The authors declare that they do not have any conflict of interest.

References:

- Ahmadi R, Oryan Sh** (2008) Effects of ovariectomy or orchidectomy and estradiol valerate or testosterone enanthate replacement on serum insulin in rats. **Pak J Biol Sci** **15**, 306-308.
- Atchley WR, Wei R, Crenshaw P** (2000) Cellular consequences in the brain and liver of age-specific selection for rate of development in mice *Genetics* **155**, 1347-1357.
- Barter ZE, Bayliss MK, Beaune PH, et al.** (2007) Scaling factors for the extrapolation of in vivo metabolic drug clearance from in vitro data: researching a consensus on values of human microsomal protein and hepatocellularity per gram of liver *Curr Drug Metab* **8**, 33-45.
- Biondo-Simões ML, Matias JE, Montibeller GR, Siqueira LC, Nunes E, Grassi CA** (2006) Effect of aging on liver regeneration in rats. *Acta Cir Bras* **21**, 197-202.
- Carlile DJ, Zomorodi K, Houston JB** (1997) Scaling factors to relate drug metabolic clearance in hepatic microsomes, isolated hepatocytes, and the intact liver: studies with induced livers involving diazepam *Drug Metab Dispos* **25**, 903-911.
- Celton-Morizur S, Desdouets C** (2010) Polyploidization of liver cells. *Adv Exp Med Biol* **676**, 123-135.
- Chang J, Hisamatsu T, Shimamura K, et al.** (2013) Activated hepatic stellate cells mediate the differentiation of macrophages. *Hepatol Res* **43**, 658-669.
- Crawford JM, Burt AD** (2012) Anatomy, pathophysiology and basic mechanisms of disease. In: *MacSween's Pathology of the liver*, 6th edition (eds Burt A, Portmann B, Ferrell L), pp. 1-74. Edinburgh: Churchill Livingstone.
- Croome KP, Segal D, Hernandez-Alejandro R, Adams PC, Thomson A, Chandok N** (2014) Female donor to male recipient gender discordance results in inferior graft

survival: a prospective study of 1,042 liver transplants. *J Hepatobiliary Pancreat Sci* **21**, 269-274.

Lopes Da Costa C, Sampaio de Freitas M, Sanchez Moura A (2004) Insulin secretion and GLUT-2 expression in undernourished neonate rats. *J Nutr Biochem* **15**, 236-241.

Davidson AJ, Castañón-Cervantes O, Stephan FK (2004) Daily oscillations in liver function: diurnal vs circadian rhythmicity. *Liver Int* **24**, 179-86.

Dijkstra CD, Döpp EA, Joling P, Kraal G (1985) The heterogeneity of mononuclear phagocytes in lymphoid organs: distinct macrophage subpopulations in the rat recognized by monoclonal antibodies ED1, ED2 and ED3. *Immunology* **54**, 589-599.

Dorph-Petersen KA, Nyengaard JR, Gundersen HJG (2001) Tissue shrinkage and unbiased stereological estimation of particle number and size. *J Microsc* **204**, 232-246.

Epstein CJ (1967) Cell size, nuclear content, and the development of polyploidy in the Mammalian liver. *Proc Natl Acad Sci USA* **57**, 327-334.

Fisher B, Gunduz N, Saffer EA, Zheng S (1984) Relation of estrogen and its receptor to rat liver growth and regulation. *Cancer Res* **44**, 2410-2415.

Friedman SL (2008) Hepatic stellate cells: protean, multifunctional, and enigmatic cells of the liver. *Physiol Rev* **88**, 125-172.

Friedman SL, Arthur MJ (1989) Activation of cultured rat hepatic lipocytes by Kupffer cell conditioned medium. Direct enhancement of matrix synthesis and stimulation of cell proliferation via induction of platelet-derived growth factor receptors. *J Clin Invest* **86**, 1780-1785.

Gandhi CR. Augmenter of liver regeneration. *Fibrogenesis Tissue Repair* 2012;5:10.

Gandillet A, Alexandre E, Holl V, et al. (2003) Hepatocyte ploidy in the normal rat. *Comp Biochem Physiol A Mol Integr Physiol* **134**, 665-673.

Gascon-Barré M, Huet PM, Belgiorio J, Plourde V, Coulombe PA (1989) Estimation of collagen content of liver specimens. Variation among animals and among hepatic lobes in cirrhotic rats. *J Histochem Cytochem* **37**, 377-381.

Gebhardt R, Mecke D (1983) Heterogeneous distribution of glutamine synthetase among rat liver parenchymal cells in situ and in primary culture. *EMBO J* **2**, 567-570.

Geerts A, Lazou JM, De Bleser P, Wisse E (1991) Tissue distribution, quantitation and proliferation kinetics of fat-storing cells in carbon tetrachloride-injured rat liver. *Hepatology* **13**, 1193-1202.

Grebely J, Page K, Sacks-Davis R, et al. (2014) The effects of female sex, viral genotype, and IL28 genotype on spontaneous clearance of acute hepatitis C virus infection. *Hepatology* **59**, 109-120.

Gressner AM, Weiskirchen R (2006) Modern pathogenetic concepts of liver fibrosis suggest stellate cells and TGF-beta as major players and therapeutic targets. *J Cell Mol Med* **10**, 76-99.

Grisham JW (2009) Organizational principles of the liver. In: *The liver: biology and pathobiology*, 5th edition (eds Arias IM, Alter HJ, Boyer JL, Cohen DE, Fausto N, Shafritz DA, Wolkoff AW), pp. 3-15. New York: John Wiley & Sons Ltd.

Gundersen HJ (1988) The nucleator. *J Microsc* **151**, 3-21.

Gupta S (2000) Hepatic polyploidy and liver growth control. *Semin Cancer Biol* **10**, 161-171.

Hall AP, Elcombe CR, Foster JR (2012) Liver hypertrophy: a review of adaptative (adverse and non-adverse) changes — conclusions from the 3rd international ESTP expert workshop. *Toxicol Pathol* **40**, 971-994.

Harkness ML, Harkness RD (1954) Further observations on collagen in regenerating liver of the rat. *J Physiol* **123**, 482-491.

Higashi N, Senoo H (2003) Distribution of vitamin A-storing lipid droplets in hepatic stellate cells in liver lobules - a comparative study. *Anat Rec A Discov Mol Cell Evol Biol* **271**, 240-248.

Hirota N, Ito K, Iwatsubo T, et al. (2001) In vitro/in vivo scaling of alprazolam metabolism by CYP3A4 and CYP3A5 in humans. *Biopharm Drug Dispos* **22**, 53-71.

Imamura H, Shimada R, Kubota M, et al. (1999) Preoperative portal vein embolization: an audit of 84 patients. *Hepatology* **29**, 1099-1105.

Jack EM, Bentley P, Bieri F, et al. (1990) Increase in hepatocyte and nuclear volume and decrease in the population of binucleated cells in preneoplastic foci of rat liver: a stereological study using the nucleator method. *Hepatology* **11**, 286-297.

Junqueira LC, Cossermelli W, Brentani R (1978) Differential staining of collagens type I, II and III by Sirius Red and polarization microscopy. *Arch Histol Jap* **41**, 267-274.

Kitagawa T, Yokoyama Y, Kokuryo T, et al. (2009) Estrogen promotes hepatic regeneration via activating serotonin signal. *Shock* **31**, 615-620.

Kmieć Z (2001) Cooperation of liver cells in health and disease. *Adv Anat Embryol Cell Biol* **161**, 1-151.

Lai JC, Feng S, Roberts JP, Terrault NA (2011) Gender differences in liver donor quality are predictive of graft loss. *Am J Transplant* **11**, 296-302.

Li Z, Tuteja G, Schug J, Kaestner KH (2012) Foxa1 and Foxa2 are essential for sexual dimorphism in liver cancer. *Cell* **148**, 72-83.

Marcos R, Monteiro RA, Rocha E (2004) Estimation of the number of stellate cells in a liver with the smooth fractionator. *J Microsc* **215**, 174-182.

Marcos R, Monteiro RAF, Rocha E (2006) Design-based stereological estimation of hepatocyte number, by combining the smooth optical fractionator and immunocytochemistry with anticarcinoembryonic antigen polyclonal antibodies. *Liver Int* **26**, 116-124.

Marcos R, Monteiro RAF, Rocha E (2012) The use of design based stereology to evaluate volumes and numbers in the liver: a review with practical guidelines. *J Anat* **220**, 303-317.

Martin G, Sewell RB, Yeomans ND, Smallwood RA (1992) Ageing has no effect on the volume density of hepatocytes, reticulo-endothelial cells or the extracellular space in livers of female Sprague-Dawley rats. *Clin Exp Pharmacol Physiol* **19**, 537-539.

Martin NC, McCullough CT, Bush PG, Sharp L, Hall AC, Harrison DJ (1992) Functional analysis of mouse hepatocytes differing in DNA content: volume, receptor expression and effect of INN γ . *J Cell Physiol* **191**, 138-144.

Massard J, Ratzliff V, Thabut D, et al. (2006) Natural history and predictors of disease severity in chronic hepatitis C. *J Hepatol* **44**, S19-24.

McCuskey RS (2006) Anatomy of the liver. In: *Zakim and Boyer's hepatology. A textbook of liver disease*, 5th edition (eds Boyer TD, Wright TL, Manns MP), pp. 3-21. Philadelphia: Saunders.

Mossin L, Blankson H, Huitfeldt H, Seglen PO (1994) Ploidy-dependent growth and binucleation in cultured rat hepatocytes. *Exp Cell Res* **214**, 551-560.

Nicol T, Veron-Roberts B (1965) The influence of the estrus cycle, pregnancy and ovariectomy on RES Activity. *J Reticuloendothel Soc* **60**, 15-29.

Oikawa H, Masuda T, Kamaguchi J, Sato S (2002) Three-dimensional examination of hepatic stellate cells in rat liver and response to endothelin-1 using confocal laser scanning microscopy. *J Gastroenterol Hepatol* **17**, 861-872.

Pandit SK, Westendorp B, Bruin A. Physiological significance of polyploidization in mammalian cells. *Trends Cell Biol* 2013;23:556-566.

Poynard T, Ratziu V, Charlotte F, Goodman Z, McHutchison J, Albrecht J (2001) Rates and risk factors of liver fibrosis progression in patients with chronic hepatitis C. *J Hepatol* **34**, 730-739.

Santos M, Marcos R, Santos N, Malhão F, Monteiro RAF, Rocha E (2009) An unbiased stereological study on subpopulations of rat liver macrophages and on their numerical relation with the hepatocytes and stellate cells. *J Anat* **214**, 744-751.

Scheicher J, Tokarski C, Marbach E, et al. (2015) Zonation of hepatic fatty acid metabolism - The diversity of its regulation and the benefit of modeling. *Biochim Biophys Acta* **1851**, 641-656.

Scotland RS, Stables MJ, Madalli S, Watson P, Gilroy DW (2011) Sex differences in resident immune cell phenotype underlie more efficient acute inflammatory responses in female mice. *Blood* **118**, 5918-5927.

Senoo H, Kojima N, Sato M (2007) Vitamin A-storing cells (stellate cells). *Vitam Hormon* **75**, 131-159.

Shimizu I, Mizobuchi Y, Yasuda M, et al. (1999) Inhibitory effect of oestradiol on activation of rat hepatic stellate cells in vivo and in vitro. *Gut* **44**, 127-136.

Shimizu I, Kohno N, Tamaki K, et al. (2007) Female Hepatology: favorable role of estrogen in chronic liver disease with hepatitis B virus infection. *World J Gastroenterol* **13**, 4295-4305.

Sirma H, Williams GM, Gebhardt R (1996) Strain- and sex-specific variations in hepatic glutamine synthetase activity and distribution in rats and mice. *Liver* **16**, 166-173.

Smith R, Jones RD, Ballard PG, Griffiths HH (2008) Determination of microsome and hepatocyte scaling factors for in vitro/in vivo extrapolation in the rat and dog. *Xenobiotica* **38**, 1386-1398.

St Aubin PM, Bucher NL (1952) A study of binucleate cell counts in resting and regenerating rat liver employing a mechanical method for the separation of liver cells. *Anat Rec* **112**, 797-809.

Tacke F, Zimmermann HW (2014) Macrophage heterogeneity in liver injury and fibrosis. *J Hepatol* **60**, 1090-1096.

Teutsch HF (1984) Sex-specific regionality of liver metabolism during starvation; with special reference to the heterogeneity of the lobular periphery. *Histochemistry* **81**, 87-92.

Teutsch HF, Schuerfeld D, Groezinger E (1999) Three-dimensional reconstruction of parenchymal units in the liver of the rat. *Hepatology* **29**, 494-505.

Tsukamoto I, Kojo S (1990) The sex difference in the regulation of liver regeneration after partial hepatectomy in the rat. *Biochim Biophys Acta* **1033**, 287-290.

Vickers AE, Lucier GW (1996) Estrogen receptor levels and occupancy in hepatic sinusoidal endothelial and Kupffer cells are enhanced by initiation with diethylnitrosamine and promotion with 17 alpha-ethinylestradiol in rats. *Carcinogenesis* **17**, 1235-1242.

Villa E (2008) Role of estrogen in liver cancer. *Womens Health* **4**, 41-50.

Vinogradov AE, Anatskaya OV, Kudryavtsev BN (2001) Relationship of hepatocyte ploidy levels with body size and growth rate in mammals. *Genome* **44**, 350-360.

Vital P, Larrieta E, Hiriart M (2006) Sexual dimorphism in insulin sensitivity and susceptibility to develop diabetes in rats. *J Endocrinol* **190**, 425-432.

Wake K (1980) Perisinusoidal stellate cells (fat-storing cells, interstitial cells, lipocytes), their related structure in and around the liver sinusoids, and vitamin A-storing cells in extrahepatic organs. *Int Rev Cytol* **66**, 303-353.

Yang K, Du C, Cheng Y, Li Y, Gong J, Liu Z (2013) Augmenter of liver regeneration promotes hepatic regeneration depending on the integrity of Kupffer cell in rat small-for-size liver transplantation. *J Surg Res* **183**, 922-928.

Yasuda M, Shimizu I, Shiba M, Ito S (1999) Suppressive effects of estradiol on Dimethylnitrosamine-induced fibrosis of the liver in rats. *Hepatology* **29**, 719-727.




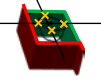
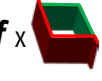


Yokoyama Y, Nagino M, Nimura Y (2007) Which gender is better positioned in the process of liver surgery? Male or female? *Surg Today* **37**, 823-830.

Figure 1: Overview of the methods used in this study in thin and thick liver sections and in frozen pieces.

Figure 2: Thin liver section immune-stained against glial fibrillary acidic protein for detecting hepatic stellate cells (HSC). The relative volume of HSC was estimated by counting points falling within HSC and within the reference space (whole liver). In order to avoid counting an excessive number of points, two different point densities were used: the sparser points (in yellow) quantified the whole liver. Bar = 4 μm .

Figure 3: Thick liver section immune-stained against glial fibrillary acidic protein and ED2 for detecting hepatic stellate cells (HSC, black arrows) and Kupffer cells (KC, open arrows), respectively. Cells were counted if their nucleus was in focus below 4 μm and above or equal to 24 μm in the z-axis (section depth), if they were inside the inclusion (green) lines, or not touching the exclusion (red) lines. Bar = 6 μm .

Figure 4: Histogram of the number weighted mean nuclear volume of hepatocytes in males (yellow) and female (blue). The volume of diploid nuclei was estimated to be $225 \pm 36 \mu\text{m}^3$, whereas that of tetraploid nuclei was $447 \pm 52 \mu\text{m}^3$.

	Thick sections						Thin sections		Pieces
Stain/Marker	GFAP-GS	GFAP	E-cadherine	E-cadherine	ED2	GFAP-ED2	Sirius red	GFAP	PI
Method		f_X 	f_X 		f_X 		++++ ++++ ++++	++++ ++++ ++++	
Assessment	Distribution of HSC	N of HSC	N of HEP	\bar{V}_N cell and HEP nuclei	N of KC	Colocalization HSC and KC	V_V collagen	V_V of HSC	ploidy

HEP: hepatocytes; HSC: hepatic stellate cells; KC: Kupffer cells; N: total number; V_V : relative volume, \bar{V}_N number weighted mean cell volume.

